Analysis on Influence of Blasting of Underlying of Tunnel on Surrounding Rock of Existing Tunnel-type Anchorage Based on Numerical and Theory Method

Wang Lianbin

China Communications 2nd Navigational Bureau 2nd Engineering Co.ltd, Chongqing, 401121, China

E-mail: xlleng@whrsm.ac.cn

Keywords: underlying tunnel; tunnel-type anchorage; blasting; loose circle; dynamic analysis

Abstract: Due to the constraints of construction period and site conditions, in order to ensure the stability of the surrounding rock of existing tunnel-type anchorage and the safety of bridge, it is necessary to study the influence of blasting construction of underlying tunnel on the surrounding rock of the existing tunnel-type anchorage. Based on the methods of numerical methods and theoretical analysis, this paper systematically analyzed the influence of underpass tunnel construction on the surrounding rock of the tunnel-type anchorage from the aspects of loose circle of the surrounding rock. The results show that when underlying tunnel blasting, the peak velocity of the top arch monitoring points in each section of the right underlying tunnel specifically is largest. For the blasting of the upper steps, it is necessary to focus on monitoring the vibration speed of the top arch. The total peak velocity of the monitoring point of the anchorage does not exceed 1 cm/s, which is smaller than the allowable vibration velocity of the particle which is stipulated by the blasting and meets the stipulated requirements. Based on the elasto-plastic theory, Hoek-Brown strength criterion is used to calculate the thickness of the loose circle of top arch about 2.04m. Therefore, the blasting of underlying tunnel has less influence on the surrounding rock of existing tunnel-type tunnel.

1. Introduction

The tunnel-type anchorage is one of the key bearing structures of the suspension bridge. Its overall stability and stress state directly affect the safety and normal use of the suspension bridge [1]. Because of the steep terrain of mountainous canyons, due to the terrain conditions of the two sides, the main towers of suspension bridges are arranged on both banks. In the shallow part of the slope, there are highway tunnels passing through the lower part. Due to the constraints of construction time, the upper tunnel-type anchorages will be constructed before the lower tunnels. In this case, the blasting construction of the tunnel will have a safety effect on the surrounding rock of the existing tunnel-type anchorages. The influence determines the long-term operation safety of the bridge. Therefore, it is of great significance to study the influence of tunnel construction on the surrounding rock of the existing tunnel-type anchorages.

With the development of western China, adjacent tunnel projects and tunnel-type anchorages have been extensively constructed, and the study on the stability and safety of tunnel blasting has received increasing attention from scholars. The study of the influence of blasting vibration on tunnels mainly includes two aspects: one is the influence of blasting vibration on adjacent tunnels, and the other is the effect of blasting vibration on the tunnel itself. This article mainly studies the first one. For the influence of blasting vibration on the surrounding rock of existing tunnels, many people have done a lot of research with reference guidance [2-6]. However, currently there are relatively few studies on the effect of construction of underlying tunnels on existing tunnel anchorage [7,8], and the analytical method is mainly limited to one of three methods: monitoring methods, numerical analysis, and theoretical analysis. They are rarely studied by two or more means. Therefore, this article will use them separately. Therefore, in this paper, numerical and theoretical methods are used to systematically study the effects of blasting of underlaying tunnels on the surrounding rock of

  DOI: 10.25236/icemit.2019.033

existing tunnel-type anchorages.

2. Engineering Situation and Numerical Model

The river valleys of a special bridge project area have an open “V” shape, and both bank slopes have step-like characteristics of steep junctions. Affected by various factors such as lithology, occurrence, and structure, the slope of the bank slope is generally from 40° to 45°, locally greater than 50°. The stratum of the bridge area is mainly permian volcanic rocks, pyroclastic rocks, and stratum of quaternary (Fig. 1). The rock types mainly include dense massive basalts, amygdaloidal basalts, and tuffs. The three-dimensional relationship between tunnel and tunnel anchor is shown in Fig. 1.

The tunnel is a centerless arch tunnel. Taking into account the geological structure and geotechnical characteristics of the bank slope, the main geotechnical considerations in the numerical analysis process are strongly weathered basalt, medium weathered basalt, and tuff rocks. The three-dimensional geomechanical model is shown in Fig. 2. The dynamic boundary conditions are: the model has free-field boundaries on the sides and the viscous boundary on the bottom. The mechanical parameters of surrounding rock are shown in Table 1.

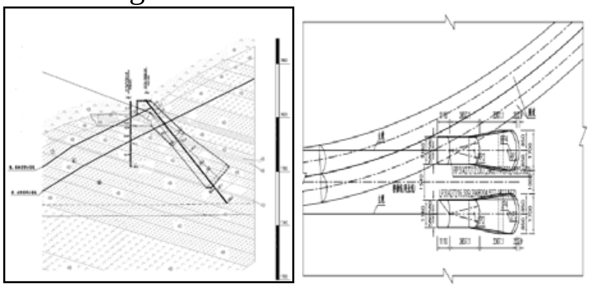

Fig. 1 Geological vertical section of right bank and plane relationship diagram between tunnel and tunnel-type anchorage

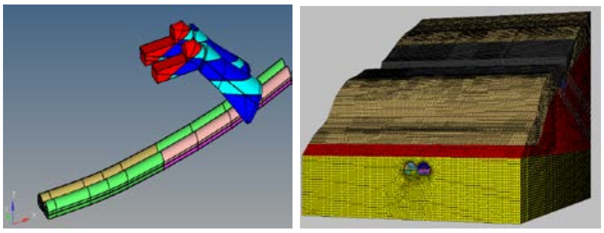

Fig. 2 Three-dimensional geomechanical model

Table 1 Mechanical parameters of rocks

Surrounding rock	Elastic modulus (GPa)	Poisson's ratio	Cohesion (MPa)	Internal friction angle (°)	Tensile strength (MPa)
Strongly weathered basalt	0.5	0.28	0.35	30	0.3
Medium weathered basalt V	2	0.27	0.5	38	0.45
Medium weathered basalt IV	4.5	0.22	0.7	40	0.65
Tuff	0.3	0.28	0.2	35	0.15

3. The influence of underlying tunnel blasting on surrounding rock of existing tunnel-type anchorage

3.1 Research scheme

Blasting is an instantaneous and complicated process. Because the explosion mechanism and influencing factors of explosives are extremely complex and measurement methods are limited, at present, numerical analysis methods are generally used. The assumed blasting input load is a triangular pulse wave [9]. The peak load is determined by (1) and (2):

$$\sigma_m = P_w(\frac{1}{\bar{r}})^{\alpha} \tag{1}$$

$$P_w = \frac{\rho_w D^2}{1+K} \tag{2}$$

where P_w is the average initial pressure (N/m2) produced by the detonation wave at the center of the drug package; $\bar{r}$ is the ratio radius($\bar{r} = R/R_w$), R is the distance from the axis of the drug package (m); R_w is the radius of the cross-section of the drug package (m), $\bar{r}$ is tentatively set to 120; αis the constant associated with rock and explosive species, generally related to the Poisson's ratio of the rock($\alpha = 2 - \frac{\mu}{1-\mu}$); ρ_w is the density of the charge.

Fig. 3 shows the design of the smooth blasting of Grade IV surrounding rock of non-middle-linked multi-arch tunnel. Table 2 shows the smooth blasting parameters of Grade IV surrounding rock of non-middle-linked multi-arch tunnel. According to equations (1) and (2), The corresponding blast peak stress is obtained in Table 2.

Table 2 Parameters for smooth blasting of underlaying tunnel

Process	Blast hole	Blast hole depth (m)	Number of Blast hole	Explosive charge in per hole (kg)	Total explosive charge (kg)	Peak load (MPa)
Step IV	Cutting hole	1.1	16	0.7	11.2	1.350
Step V	1st, 2st and 3st rows	0.8	13	0.3	3.9	0.796
Step VI	1st, 2st and 3st rows	0.8	11	0.3	3.3	0.796

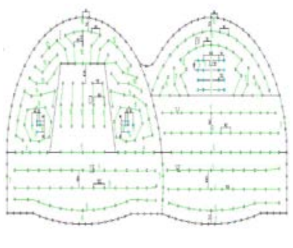

Fig. 3 Blast holes layout for smooth blasting of underlaying tunnel and detonation network diagram

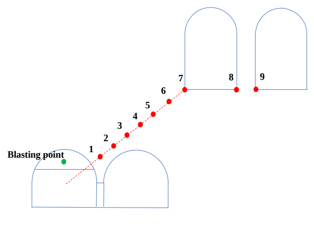

Fig. 4 Connection of underlaying tunnel and tunnel-type anchorage and monitoring points layout of anchorage

In order to study the maximum impact of blasting of the left tunnel on the tunnel anchorage, the left tunnel face is excavated to the corresponding position at the bottom of the 31.3m front of anchor plug of the tunnel-type anchor. It can be seen from Table 2 that the peak load of the blasting load in Step IV of the left tunnel is the highest, and the step is to excavate up the stairs, which is closest to the tunnel-type anchorage, so this step is the load acts as an input load to the model. Fig. 4 shows the layout of monitoring points for the tunnel and tunnel-type anchorage lines and anchor plug. In addition, monitoring points such as the top arch, side wall, and invert at the position of the blasting surface at 10 m and 20 m before and after the right tunnel are also arranged.

3.2 Calculation result analysis

3.2.1 The right tunnel

Fig. 5-8 shows the velocity time histories and velocity peaks at the monitoring points of the top arch, side wall and invert of the right tunnel at the location of the blasting surface and at 10m and 20m before and after blasting surface. The following conclusion can be drawn from the figure.

(1) The velocity waveforms of different directions in the right tunnel are not the same. The velocity waveforms in the z direction basically show a regular triangle wave, while the velocity waveforms in the x direction and y direction basically show a positive and negative triangle wave; inverts, side walls and top monitoring points have basically the same velocity pattern.

(2) The peak velocity of the monitoring points in each section of the right tunnel is specifically: top arch>invert >sidewall, which is more obvious in the y direction. Therefore, for the excavation of the upper bench, the vibration velocity of the top arch is mainly monitored.

(3) In the blasting direction and receding direction of the blasting surface, the peak speeds of the top arch, side wall and inverts in the x direction increase as the excavation distance increases. However, the increasing magnitude in the receding direction is smaller than that in the blasting direction. This is because tunnel blasting is carried out along the direction of excavation. At the same time, only blasting is done on the upper bench and the tunnel is curved; The peak speeds of the inverts and the side walls in the y direction are basically the same within 20m before and after the blasting surface, while the top arches in the direction of tunnel excavation and the backward direction is substantially reduced with the distance from the blasting surface increasing. Compared with the blasting surface, the peak velocity reduction reached around 80%; In the z-direction, the peak velocity of the top arch, side wall, and invert is basically the same as the distance in the driving direction, and the velocity reaches the maximum near the blasting surface excavation direction, while in the backward direction, it gradually decreases as the distance from the blasting surface increase; The total peak speed is similar to the peak speed in the z direction.

3.2.2 The lines between tunnel and tunnel-type anchorage and tunnel-type anchorage

Fig. 9 is the relationship between the peak speed of the monitoring points and the distance the connecting between tunnel and tunnel-type anchorage and tunnel-type anchorage. The number of the monitoring points is compiled from the nearest to the far end of the tunnel, and the monitoring points 1-6 are the equidistant monitoring points of the connection between the tunnel and the tunnel-type anchorage, and the monitoring points 7-9 are the bottom and the middle of the 31.3m section of the anchor plug, as shown in Fig. 4. It can be seen from Fig. 9 that the blasting seismic wave sharply attenuates in the area closer to the blast source and flattens in the far area, and the peak speed reduction in all directions is relatively large. For example, the peak speed of the monitoring point 2 has been reduced to about 50% of monitoring point 1 and peak speed of monitoring point 6 only accounts for about 13% of monitoring point 1. For the total peak velocity, the peak velocity of the monitoring points 7-9 of the anchor plug does not exceed 1 cm/s. According to the provisions of the “Blasting Safety Regulations” (GB6722-2014), the particle velocity of the traffic tunnel is allowed to be 15-20cm/s. Therefore, the blasting vibration velocity is less than the requirements specified in the safety regulations for blasting, which can reduce the influence of blasting vibration on the stability of tunnel surrounding rock and the impact on the concrete structure of the second liner.

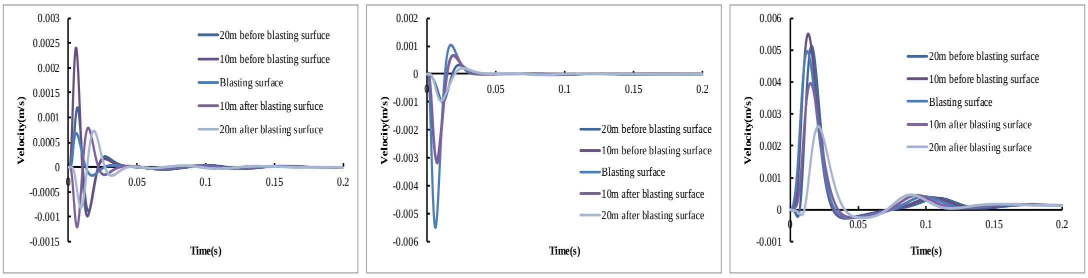

(a)x direction (b)y direction (c)z direction

Fig. 5 Velocity time history of top arch monitors in right underlaying tunnel

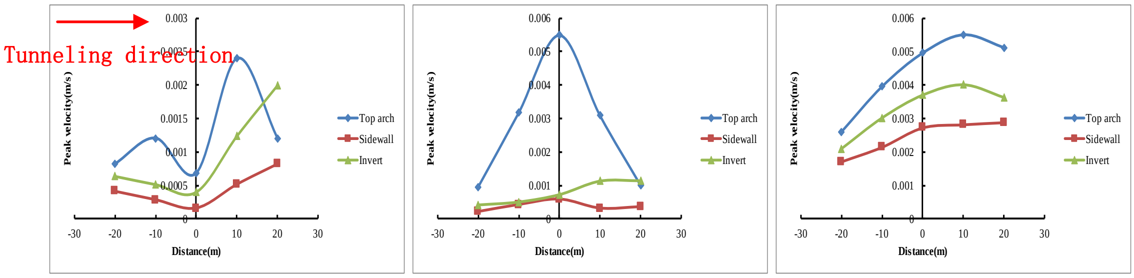

(a)x direction (b)y direction (c)z direction

Fig. 6 Relationship between peak velocity of monitoring points and distance in right underlaying tunnel

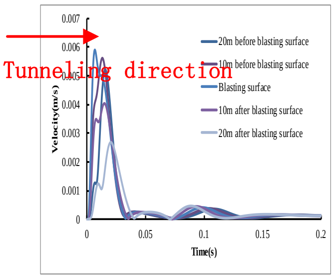

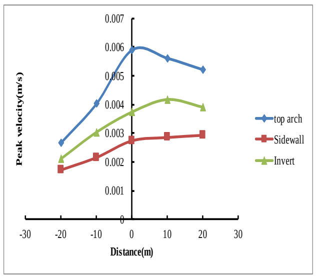

Fig. 7 Total velocity time history of top arch monitors in right underlaying tunnel

Fig. 8 Relationship between total peak velocity of monitoring points and distance in right underlaying tunnel

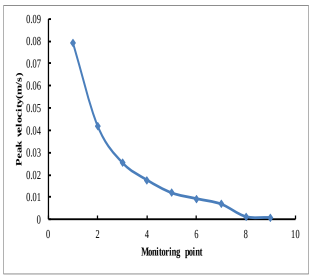

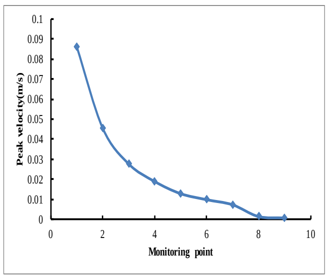

(a) z direction (b) total peak velocity

Fig. 9 Relationship between peak velocity of monitoring points and distance in the connecting between tunnel and tunnel-type anchorage and tunnel-type anchorage

4. Loose circle analysis

4.1 Initial judgment for loose circle

According to the size of the loose circle radius, the surrounding rocks are divided into small loose zone, middle loose zone and large loose zone. The surrounding rock in small loose zone is stable, and the loose rock in the middle ring is generally stable, while the surrounding rock in the large loose zone is unstable. The provisions of the size of the loose circle are given in literature [10]. Table 3 is the maximum thickness of the loose circle of surrounding rock under the maximum single-stage initiation dosage of existing projects. It can be found that the maximum loosening ring thickness in Table 3 basically conforms to the classification condition of the loose ring theory. It can be generally stated that the maximum loosening ring thickness of the surrounding rock can be preliminarily determined according to the loosening ring theory. The type of surrounding rock of this project is IV~V, so the maximum loosening thickness of the wall rock does not exceed 3m under the maximum single-stage explosive charge of 11.2kg.

Table 3 The maximum thickness of the loose circle of surrounding rock under the maximum single-stage initiation dosage of existing projects

Engineering	Lithology	The maximum thickness of loose circle (m)	Literature	Engineering	Lithology	The maximum thickness of loose circle (m)	Literature
Hepingxia tunnel	IV	2	[11]	Mine roadway of Shizishan	III	1.35	[15]
	V	2.4		Heshang tunnel		1.8	[16]
A mine transport lane		1.8	[12]	Heluoshan tunnel	IV	2.5	[17]
Underground powerhouse in right bank of Wudongde hydropower station		1.2	[13]	double line tunnel of Niuwanggai	IV	1.5	[18]
Diversion tunnel of Jinxiang Hydropower Station		1.7	[14]	tunnel anchorage in Yichang bank of Sidu river bridge		<4	[19]

4.2 Theoretical Formula for Loose Ring

Based on the calculation of elastic-plastic theory, the Hoek-Brown criterion is used to calculate the thickness of rock loose ring [20]. Its basic assumptions: the tunnel has a circular cross-section and the properties of the surrounding rock are the same in the infinitely long tunnel length; the surrounding rock is a homogeneous, isotropic linear elastic body with no creep or viscous behavior; The initial ground stress is self-gravity stress and is an isotropic pressure state (ie, the assumed side pressure coefficient is 1). Then the hoop plastic stress is

$$\sigma_\theta^p = \frac{\sigma_{ci}}{m_b}\left[m_b(1-a)\ln\left(\frac{r}{r_0}\right)+\left(m_b\frac{P_i}{\sigma_{ci}}+s\right)^{(1-a)}\right]^{\frac{1}{1-a}} - \frac{\sigma_{ci}}{m_b}s + \sigma_{ci}\left[m_b(1-a)\ln\left(\frac{r}{r_0}\right)+\left(m_b\frac{P_i}{\sigma_{ci}}+s\right)^{(1-a)}\right]^{\frac{a}{1-a}} \quad (3)$$

According to the definition of the loose zone: The tangential stress on the boundary of the loose zone is the initial stress P_0, and the radius R of the loose zone can be found by entering the formula above. Where m_b, s, σ_{ci}, a are the properties of the rock itself, which can be solved according to (4)-(6), respectively; P_i is the supporting force; r is the distance from the center of the tunnel, ie the radius of the loose ring; r_0 is the radius of the tunnel.

$$m_b = \exp\left(\frac{GSI-100}{28-14D}\right)m_i \tag{4}$$

$$s = \exp\left(\frac{GSI-100}{9-3D}\right) \tag{5}$$

$$a = 0.5+\frac{1}{6}\left[\exp\left(\frac{-GSI}{15}\right)-\exp\left(\frac{-20}{3}\right)\right] \tag{6}$$

where *GSI* is a geological strength index, which can be solved according to the modified *GSI* method ((7)) and (8) [21]. *D* is the perturbation parameter and the range of value is 0-1, depending on the degree of disturbance of the in-situ rock mass by external factors.

$$GSI = RMR - 5 \tag{7}$$

$$BQ = 170\ln\frac{15+0.24RMR}{5.7-0.06RMR} \tag{8}$$

According to the “Code for Design of Highway Tunnels (JTGD70-2004)”, the ratio of the load released by surrounding rock and initial support in Type IV surrounding rock is from 60% to 80%, and the initial support takes 80% of the surrounding rock pressure. Surrounding rock pressure is

$$q = 0.45\times 2^{S-1}\times \gamma\omega \tag{9}$$

$$\omega = 1+i(B-5) \tag{10}$$

Where *S* is the grade of surrounding rock, *B* is the tunnel width. When *B*> 5m, *i* takes 0.1. Therefore, according to the basic parameters of the project, the radius of the top arch loose circle by substituting (3) can be calculated as R0=7.54m. The thickness of the loose ring in the roof is:

$$D = R_0 - r = 7.54 - 5.5 = 2.04m \tag{11}$$

Therefore, relative to the spatial distance between the underlying and the existing tunnel-type anchorage, the loose loop thickness generated by the tunnel blasting construction has little effect on the surrounding rock of the existing tunnel-type anchorage.

The above process can accurately calculate the thickness of the loose zone of the surrounding rock in the circular tunnel. However, the selection of calculation parameters, especially the accuracy of the values of *m*, *s*, *a*, and *D* of the surrounding rock, needs to be improved. Because the cross-section of the tunnel in this project is not circular, and the initial stress of the surrounding rock has obvious directionality, the distribution of the loose ring in the cross section is irregular, showing the tendency that the thickness of the loose ring in the dome is greater than that in the horizontal direction. Therefore, the thickness of loosening ring calculated in this paper is also a semi-empirical and semi-theoretical derivation.

Acknowledgment

The work reported in this paper is financially supported by the National Natural Science Foundation of China (No. 51679232, No. U1402231) and the National Key Basic Research Program of China (973 Program) under Grant No. 2015CB057905. The authors are thankful for these supports.

References

[1] A. Wu, Y. Peng, Z. Huang, J Zhu, “Rock mechanics comprehensive study of bearing capacity characteristics of tunnel anchorage for super-large span suspension bridge, ” Chinese Journal of Rock Mechanics & Engineering, vol. 29, pp. 433- 441, March 2010.

[2] X. Xie, “Study on dynamic effects of existing tunnel caused by blasting excavation of undercrossing new tunnel,” Changsha: Changsha University of Science & Technology, 2013.

[3] L. Cai, F. Zhu, L. Wu, F Hang, S Peng, “Influence of blasting vibration of lower water supply tunnel on the excavation of upper tunnel,” Highway Engineering, vol. 40, pp. 28-32, March 2015.

[4] D. Zhao, M. Wang, “Study on influence of blasting vibration on cross tunnels with small clearance,” Chinese Journal of Geotechnical Engineering, vol. 29, pp. 116-119, January 2007.

[5] P. Ye, X. Yang, B. Ling, Y. Zhang, “Vibration effects on existing tunnel induced by blasting of an adjacent cross tunnel,” Rock and Soil Mechanics, vol. 32, pp. 537-541, February 2011.

[6] L. Yuan, C. Tang, J. Zhu, Y. Bai, “Control blasting technology of expressway tunnel underpass existing railway tunnel,” Engineering Blasting, vol. 22, pp. 64-67, January 2016.

[7] J. Peng, Q. Zhang, H. Hu, S. Long, “Surrounding rock structures and mountain stability of chadong bank of the Aizhai suspension bridge,” Journal of Chongqing Jiaotong University (Natural Science), vol. 30, pp. 1298-1302, June 2011.

[8] Z. Dong, Q. Zhang, X. Ding, L. Zhang, “Numerical analysis of rockmass stability in tunnel anchoring of Aizhai bridge,” Journal of Yangtze River Scientific Research Institute, vol. 22, pp. 54-58, June 2005.

[9] X. Xia, J. Li, H. Li, Y. Liu, Q. Zhu, “Udec modeling of vibration characteristics of jointed rock mass under explosion,” Rock and Soil Mechanics, vol. 26, pp. 50-56, January 2005.

[10] F. Dong, H. Song, Z. Guo, S. Lu, S. Liang, “Roadway support theory based on broken rock zone,” Journal of China Coal Society, vol. 19, pp. 21-31, January 1994.

[11] S. Huan, H. Zhou, X. Deng, D. Liu, X. Wang, “Measured analysis and application of loose circle in surrounding rock of long - span tunnel with layered rock mass,” Journal of China & Foreign Highway, vol. 34, pp. 246-249, April 2014.

[12] H. Wang Haibo, Y. Xu, “Testing and analysis of influence of blasting on soft rock roadway loose zone,” Safety in Coal Mines, vol. 43, pp. 198-2000, November 2012.

[13] X. Zhang, J. Yin, X. Ren, “Test and analysis of loose circle of powerhouse surrounding rock in blasting excavation,” Yangtze River, pp. 36-39, November.

[14] J. Xiao, X. Feng, D. Lin, “Influence of blasting round on excavation damaged zone of surrounding rock,” Chinese Journal of Rock Mechanics & Engineering, vol. 29, pp. 2248-2255, November 2010.

[15] J. Yang, X. Sun, C. Shi, C. Shi, Li He, “The study on evolution law and thickness test of broken rock zone of deep roadway surrounding rock,” Yunnan Metallurgy, vol. 46, pp. 18-23, February 2017.

[16] Y. Zhou, C. Wu, Q. Zhang, ‘Test analysis on the broken rock zone of the surrounding rock blasting for tunnel,” Mining Technology, vol. 5, pp. 63-64, March 200.

[17] Z. Shen, H. Fu, X. Zhao, “Study on range of broken rock zone of blast-constructing single line railway tunnel,” Engineering Blasting, vol. 16, pp. 32-36, March 2010.

[18] H. Fu, Y. Zhao, J. Xie, “Test analysis on the broken rock zone of the surrounding rock blasting for railway double-line tunnel,” China Railway Science, vol. 31, pp. 54-58, May 2010.

[19] J. Wang, “Project examples on broken rock zone of the surrounding rock blasting for chamber using geophysical methods,” Resource Environment & Engineering, vol. 22, pp. 82-84, December 2008.

[20] R. Wang, D. Yuan, J. Zhang, J. Yang, “Analysis on broken zone of surrounding rock in tunnel based on Hoek-Brown strength criterion,” Journal of Safety Science and Technology, vol. 13, pp. 58-63, March 2017.

[21] H. Xu, F. Chen, B. Wang, Z. Hua, H. Gen, “Relationship between RMR and BQ for rock mass classification and estimation of its mechanical parameters,” Chinese Journal of Geotechnical Engineering, vol. 36, pp. 195-198, January 2014.